

Mechanical and thermal behaviors of silica-based porous ceramics by addition of silicon carbide

Jeong-Gu Yeo^{a,*}, Young-Hwan Kim^{a,b}, JeongSoo Park^a and Sung-Churl Choi^{b,*}

^aKorea Institute of Energy Research, 152 Gajeong-ro, Yuseong-gu, Daejeon 34129, Korea

^bDivision of Materials Science & Engineering, Hanyang University, 222 Wangsimni-ro, Seongdong-gu, Seoul 04763, Korea

The mechanical and thermal behaviors of porous silica-based ceramic cores for preformation of internal cooling passages in gas turbine blades were studied. The silica-based ceramic cores are composed of fused silica and zircon powders, and silicon carbide powder (SiC) was added to improve the mechanical and thermal properties of the silica-based ceramic cores. Cristobalite, which was formed by crystallization of amorphous silica on SiC surface, improved the flexural strength, bulk density and thermal conductivity of silica-based ceramic cores up to an addition of 10 wt% SiC. The SiC on the silica-based ceramic cores enhanced the thermal conductivity, because SiC has higher thermal conductivity compared with matrix materials of ceramic cores (fused silica and zircon). However, in case of 20 wt% SiC on ceramic core, the crystallization of fused silica was accelerated due to SiC addition which acts as a seed of crystallization, therefore, many microcracks were generated by phase transformation ($\beta \rightarrow \alpha$) of cristobalite. As a result, the flexural strength, relative density and thermal conductivity of the ceramic core with 20 wt% SiC were reduced.

Key words: Ceramic core, Fused silica, Porous ceramics, Silicon carbide, Thermal conductivity.

Introduction

Fused silica (SiO_2) has frequently been used in steel industries because of its good refractoriness. It has also been used to make ceramic cores for forming internal cooling passages in gas turbine blades [1, 2] due to its high temperature stability and low thermal expansion ($0.55 \times 10^{-6}/\text{K}$) [3]. Despite these advantages, fused silica has a low thermal conductivity of $1.3 \text{ W/m} \cdot \text{K}$ [4], which may generate a temperature difference between the surface and internal material. Recently, there are many researches for preparation and characterization of silica-based ceramic cores. Kazemi et al. investigated that the effect of zircon on silica-based ceramic cores [5]. They reported that the zircon does not significant effect on crystallization of fused silica on silica-based ceramic cores. Moreover, Kim et al. reported that the effect of NaOMe addition on ceramic cores [6].

SiC has been used in structural applications [7, 8] due to its chemical inertness and excellent high-temperature properties. In particular, single-crystal SiC has a higher thermal conductivity ($490 \text{ W/m} \cdot \text{K}$) than oxide ceramics such as fused silica (amorphous SiO_2 , $1.3 \text{ W/m} \cdot \text{K}$), cristobalite (crystalline SiO_2 , $6.15 \text{ W/m} \cdot \text{K}$), zircon flour (ZrSiO_4 , $3.5 \text{ W/m} \cdot \text{K}$), and alumina (Al_2O_3 , $18 \text{ W/m} \cdot \text{K}$) [9–11]. Barea et al. [12] reported

that the thermal conductivity of dense alumina increased with the addition of the SiC. They obtained an enhanced thermal conductivity ($50 \text{ W/m} \cdot \text{K}$) compared to pure alumina ($30 \text{ W/m} \cdot \text{K}$) at room temperature with the addition of 30 vol% SiC. Thus, it is expected that the thermal conductivity of silica-based ceramics would be improved by the addition of SiC.

In the present study, the thermal conductivity of porous silica-based ceramic cores containing SiC was estimated using a laser-flash technique. In addition, by comparing porous ceramic cores and hot-pressed specimens that had high density, the effect of pores on the thermal conductivity was evaluated. Moreover, the microstructure, crystal structure, flexural strength, and density were measured.

Experimental Procedure

The fused silica was used as matrix materials of silica-based ceramic cores, and its compound consisted of coarse and fine powders. The coarse fused silica had broad particle sizes of 25 to $150 \mu\text{m}$ (99.6% purity, Boram Chemetal, Korea), and the fine fused silica was composed of two types of powders with D_{50} values of $5 \mu\text{m}$ (99.7% purity, Sibelco, Belgium) and $0.3 \mu\text{m}$ (99.8% purity, Denka, Japan). In addition, zircon flour (97.5% purity, $1 \mu\text{m}$, Cenotec, Korea), which prevent shrinkage of ceramic cores on sintering and enhance dimensional stability during investment casting, was used as another matrix material and SiC (97.5%, 400 mesh, Sigma-Aldrich, USA) was used as an additive. The batch of powders is listed in Table 1.

*Corresponding author:

Tel : +82-42-860-3744, 82-2-2220-0505

Fax: +82-42-860-3133, 82-2-2291-6767

E-mail: jgyeo@kier.re.kr, choi0505@hanyang.ac.kr

Table 1. The compositions of K0, K5, K10 and K20 (wt%).

Sample batches	Fused silica (wt%)	Zircon flour (wt%)	SiC (wt%)
K0	75.00	25.00	0
K5	71.25	23.75	5
K10	67.50	22.50	10
K20	60.00	20.00	20

Paraffin wax (M.P. 69 °C, Nippon-Seiro, Japan) and microcrystalline wax (M.P. 82 °C, Nippon-Seiro, Japan), oleic acid (C₁₉H₃₄O₂, Samchun Pure Chemical, Korea), and stearic acid (C₁₉H₃₆O₂, Samchun Pure Chemical, Korea) were used to prepare the thermoplastic binders. The waxes were used as main binders, and the acids were used as lubricants. All batches of silica-based ceramic cores contained 20 wt% of thermoplastic binders.

To prepare slurries for making green bodies of ceramic cores, individual batches of raw ceramic powders were ball-milled for 6 hrs. After then, the melted thermoplastic binders were added to the ceramic powders continued for 2 additional hrs at 90 °C. The slurries were fed for making green bodies into rectangular bars with dimensions of 25 × 90 × 13 mm (W × L × H) and cooled to room temperature. The green bodies were inserted into a fine fused silica powder bed before heat treatment. During heat treatment, the green body could collapse due to melting of the thermoplastic binders. The green bodies with a powder bed heated for debinding and sintering, using a box furnace at 1,200 °C for 2 hrs under air atmosphere, to make the porous silica-based specimens. To compare the effects of pores on thermal conductivity, the powders, which have same composition with porous silica-based ceramic core, were hot-pressed under an inert gas atmosphere to fabricate the high-density specimens. The powders were hot-pressed preparing at 1,200 °C for 1 hr at 30MPa uniaxial pressure.

To measure oxidation rate of SiC, the powder compounds before mixed with thermoplastic binders were analyzed using thermogravimetry/differential thermal analysis (TG/DTA, SDT 2960 Simultaneous, TA instruments, USA). The 3-point flexural strength of the samples was measured using a universal testing machine (UTM, H10SK, Hounsefield, England) with span size of 80 mm and crosshead speed of 1 mm/min according to ASTM C1674-11 [13]. The X-ray diffractometer (XRD, D/Max-2200, Rigaku, Japan, $\lambda_{\text{CuK}\alpha} = 1.54178 \text{ \AA}$) was used to confirm the phase transformation. The microstructures of the silica-based ceramic cores were observed by field-emission scanning electron microscopy (FE-SEM, S-4800, Hitachi, Japan). The bulk and apparent porosities were determined by applying Archimedes method, while the relative density was calculated using the rule of mixtures. To measure the thermal diffusivity and thermal conductivity, pellets with a diameter of 12.7 mm and a thickness of 1.5 mm were

evaluated using a laser-flash analyzer (LFA, LFA-427, Netzsch, Germany) under an argon gas atmosphere in the temperature range of 25 to 1,000 °C. The surfaces of the pellet specimens were coated with carbon spray to prevent laser transmission [14]. The thermal conductivities of the specimens were calculated using equation (1),

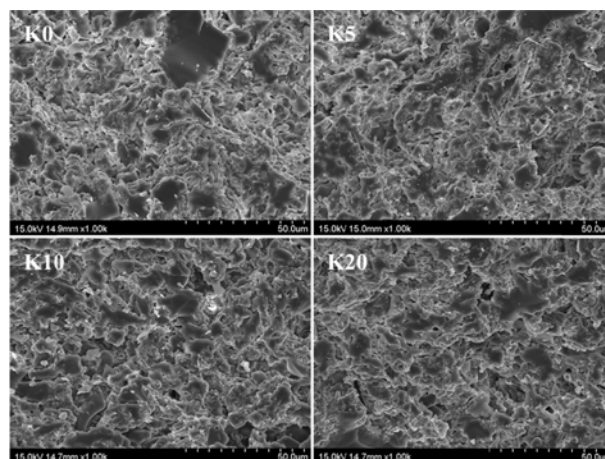
$$k = \rho \cdot C_p \cdot \lambda \quad (1)$$

where k is the thermal conductivity, ρ is the apparent density obtained using the Archimedes method, C_p is the specific heat, and λ is the thermal diffusivity that was measured by a laser-flash analyzer.

Results and Discussion

To compare the microstructures of silica-based ceramic cores with SiC addition, fracture surfaces were observed using FE-SEM (Fig. 1). The ceramic cores possess many pores that were created by the evaporation of thermoplastic binders during heat treatment. There were no significant changes of microstructures as the increase of SiC content.

The fused silica was densified by viscous flow [3]. However, the fused silica occasionally crystallized to cristobalite during heat treatment. Generally, the crystallization (or devitrification) of fused silica occurs through heterogeneous nucleation, which caused by impurities, grain boundaries and dislocations [15, 16]. Wang et al. [17] and Kazemi et al. [18] reported the cristobalite and alumina addition on silica-based ceramic cores acts as a seed of fused silica crystallization, respectively. Moreover, Breneman et al. investigated that the residual quartz on fused silica enhanced the crystallization of fused silica [19]. The fused silica has amorphous (glass) phase, and therefore, the cristobalite (crystal phase) can prevent the crack propagation of fused silica. In present research, it is assumed that the SiC plays a role of the seed for crystallization of the fused silica on silica-based ceramic cores. Therefore,

**Fig. 1.** Microstructures of porous silica-based ceramic cores.

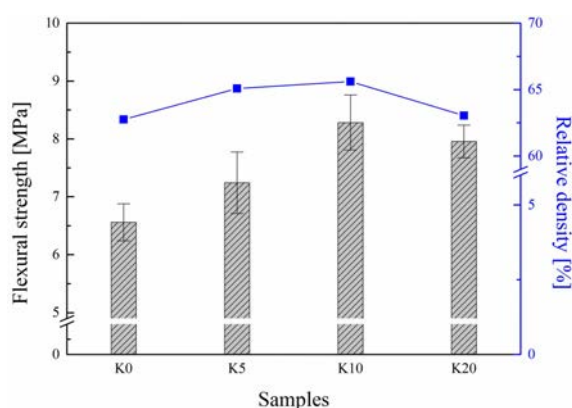


Fig. 2. Flexural strength and relative density of silica-based ceramic cores.



Fig. 3. Microcracks on fused silica by phase transformation.

the crystallization of fused silica by addition of SiC improved the flexural strength of silica-based ceramic cores. As shown Fig. 2, the flexural strength and relative density of ceramic cores were increased up to a SiC content of 10 wt% due to cristobalite on fused silica (glass phase).

In contrast, the flexural strength and relative density of K20 were reduced. It is because that the β to α -phase transformation of cristobalite. As mentioned, the flexural strength of silica-based ceramic cores were increased up to 10 wt% of SiC addition, because the cristobalite restricted crack propagation. However, the excess cristobalite on silica-based ceramic cores caused decline of the flexural strength and densification by β to α -phase transformation of cristobalite during cooling. The β -cristobalite, which crystallized from fused silica on high temperature, was transformed to α -phase between 200 °C and 300 °C. The phase transformation of cristobalite caused volume contraction, and therefore, the microcracks can be generated on its surfaces (Fig. 3). Bae [15] and Breneman [19] investigated the relationship between the cristobalite content and flexural strength of fused silica. They reported that the flexural strength of fused silica decreased with over certain amount of cristobalite, because microcracks were generated by β to α phase

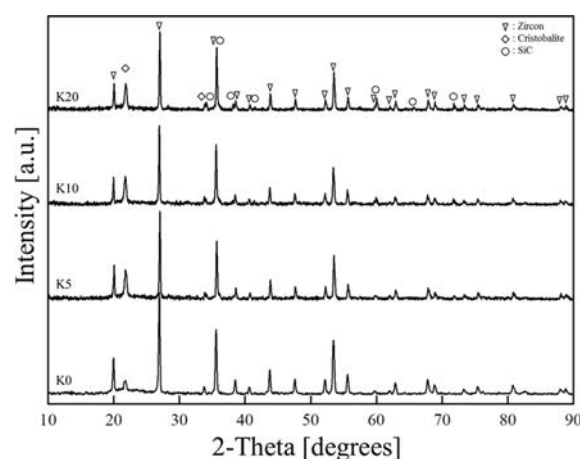


Fig. 4. XRD patterns of silica-based ceramic cores.

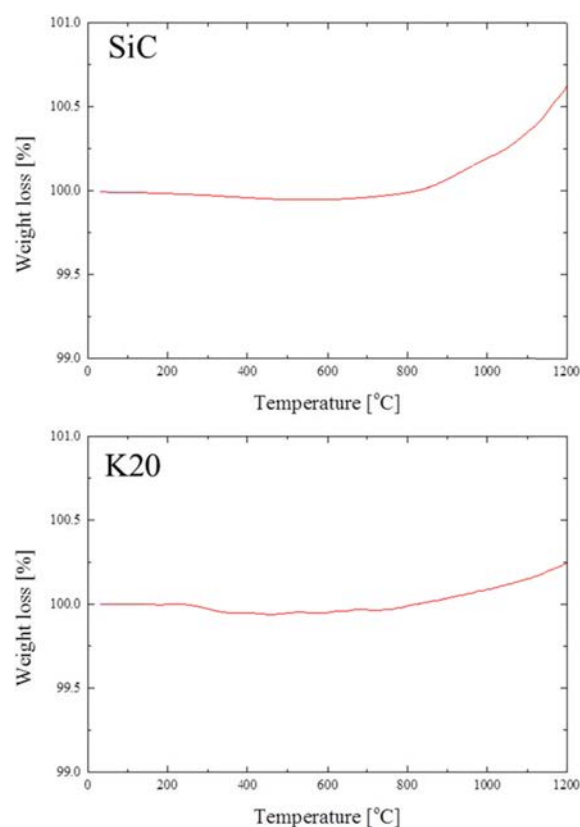


Fig. 5. Thermogravimetry analysis of SiC and K20 powders.

transition of cristobalite. Likewise, in present research, the flexural strength of silica-based ceramic cores decreased with over certain amount of SiC acted as a seed of fused silica crystallization. Therefore, in case of K20, it is considered that the effect of microcracks, which generated by phase transition of cristobalite, predominated over the restriction effect of crack propagation by cristobalite on fused silica.

The increase of cristobalite content can confirm with peaks on XRD patterns. As shown Fig. 4, the cristobalite peak intensity grew up with increase of SiC content. K0, K5 and K10 has relatively lower

cristobalite peak ($2\theta = 21.98^\circ$) compared with peak of zircon ($2\theta = 20.05^\circ$), in contrast, only the cristobalite peak of K20 is higher than a peak of zircon. Therefore, it is considered that K20 included relatively higher content of cristobalite compared to other specimens. Consequently, excess SiC addition on K20 accelerated the crystallization of fused silica, and therefore, the flexural strength and relative density decreased due to many microcracks by phase transformation of cristobalite.

To calculate oxidation rate of SiC, SiC powder and silica-zircon powder with 20 wt% SiC (K20) without thermoplastic binders were analyzed using TG/DTA under air atmosphere (Fig. 5). The weight percent of SiC increased up to 100.6%. The molar weight of SiC and SiO_2 are 40 g/mole and 60 g/mole, respectively. Therefore, the oxidation rate of SiC on K20, which was heat-treated at 1200 °C under air atmosphere, was calculated 0.4%. Meanwhile, the weight percent of K20 increased up to 100.2%. In theory, weight increase of K20 should be 0.12% because K20 has only 20 wt% SiC. However, K20 was gained 0.24% of weight increase, and it means that the additional weight of 0.12% was gained. It means 0.08% of SiC was oxidized additionally. In case of K20, the SiC powders were surrounded with oxide powders, such as fused silica and zircon. As a result, it is assumed that 0.16, 0.08 and 0.04% of SiC on K20, K10 and K5 were oxidized, by air atmosphere and other oxides during heat treatment, respectively.

Few structural models have been used to explain the effect of porosity on thermal conductivity. The Maxwell-Eucken model is often used to predict the thermal conductivity of multi-phase materials [3]. According to the model, the thermal conductivity of multi-phase materials can be estimated as follows:

$$k_m = k_c \frac{1 + 2v_d \left(1 - \frac{k_c}{k_d}\right) \left(1 + \frac{k_c}{k_d}\right)}{1 - v_d \left(1 - \frac{k_c}{k_d}\right) \left(1 + \frac{k_c}{k_d}\right)} \quad (2)$$

where k_m is the thermal conductivity of the multi-phase material, k_c is the thermal conductivity of the connected phase material, k_d is the thermal conductivity of the dispersed phase material, and v_d is volume fraction of the dispersed phase material. In the case of $k_c < k_d$, the equation to calculate the thermal conductivity of multi-phase materials can be obtained by equation (2) as follows.

$$k_m \approx k_c \left[\frac{(1 + 2v_d)}{(1 - v_d)} \right] \quad (3)$$

In the present study the theoretical thermal conductivities of the ceramic cores were calculated using the Maxwell-Eucken model (equation (3)). The theoretical thermal conductivity of silica-based ceramic cores was calculated and then, the theoretical thermal conductivities of the

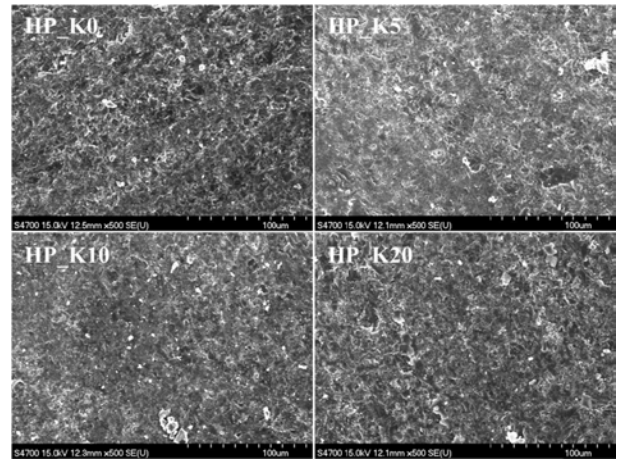


Fig. 6. Microstructures of hot-pressed specimens.

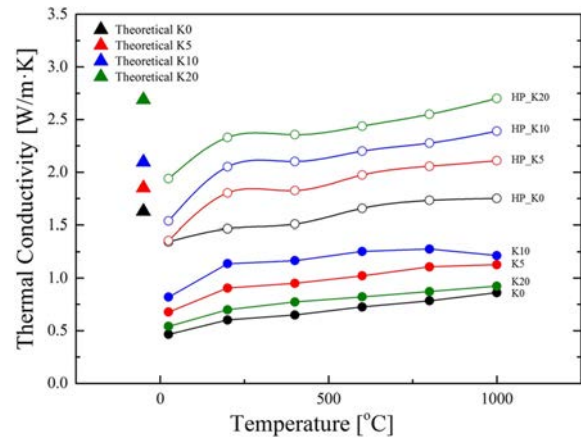


Fig. 7. Thermal conductivities of porous silica-based ceramic cores and hot-pressed specimens.

specimens containing SiC. In these calculations, SiC was the dispersed phase and silica-based ceramic was the connected phase. Moreover, the amount of oxidized SiC, which calculated as above, was adjusted on calculation of thermal conductivity. The calculated theoretical thermal conductivities of the specimens containing 0, 5, 10, and 20 wt% SiC were 1.627, 1.851, 2.096, and 2.687 W/m · K, respectively.

To compare effects of pores on thermal conductivity, the hot-pressed specimen (HP_K), which has same composition with silica-based ceramic cores as Table 1, were prepared. Specimens were hot-pressed at 1200 °C for 1 hr at 30 MPa under Ar gas atmosphere. As shown Fig. 6, the hot-pressed specimens had few pores (under 5% porosity). The thermal conductivities of the hot-pressed specimens and porous (under 30% porosity) silica-based ceramics are shown in Fig. 7. The thermal conductivities of the hot-pressed specimens steadily improved as the SiC content increased. This is because the addition of SiC, which has a higher thermal conductivity than fused silica and zircon, enhanced the thermal conductivity of the silica-based specimens. Meanwhile, it is considered that the thermal conductivities of the hot-pressed specimens were lower than the theoretical values

due to its pores. It is because that the air in the pores, which has a very low thermal conductivity, reduced the thermal conductivity of the specimens [3,11]. The measured thermal conductivities of the hot-pressed specimens containing 0, 5, 10, and 20 wt% SiC were 1.343, 1.356, 1.538, and 1.938 W/m · K, respectively, at room temperature. As a result, it is considered that the addition of SiC improved the thermal conductivity of hot-pressed specimens that had only a few pores. On the other hand, the silica-based ceramic cores were lower thermal conductivities than the hot-pressed specimens. Because the silica-based ceramic cores have many pores compared with hot-pressed specimens, and therefore, the thermal conductivity of ceramic cores were reduced. As mentioned, the pores contained air, which has low thermal conductivity, prevent thermal conduction on silica-based ceramic cores.

The thermal conductivity of silica-based ceramic cores have similar tendency with the flexural strength and relative density. The SiC addition on silica-based ceramic cores enhanced the thermal conductivity, although the ceramic cores include many pores. 10wt% SiC addition on ceramic core (K10) increased from 0.465 (K0) to 0.819 W/m · K at room temperature. However, the thermal conductivity of K20 decreased to 0.541 W/m · K. As referred to earlier, it is assumed that a high content of SiC accelerates crystallization of fused silica, and therefore, there are many microcracks by the β to α phase transformation of cristobalite during cooling. Microcracks caused empty space on particles (or grains), therefore, the thermal conduction should be prevented. Consequently, the addition of 20 wt% SiC on silica-based ceramic core reduced mechanical and thermal properties due to the excessively high content of cristobalite on ceramic cores.

Conclusions

In this study, the mechanical and thermal behaviors of silica-based ceramic cores with the addition of SiC were studied. SiC improved the mechanical properties with the addition of up to 10 wt% SiC on the silica-based ceramic cores. It is because the SiC acts as a seed of crystallization of fused silica, and therefore, the cristobalite prevents crack propagation of silica-based ceramic cores. However, excess amount of SiC reduced the mechanical properties of silica-based ceramic cores. 20 wt% SiC accelerated crystallization of fused silica, and therefore, many microcracks were generated by β to α phase transition of cristobalite. As a result, a lot of microcracks reduced the flexural strength and relative density of silica-based ceramic cores.

The SiC improved the thermal conductivity of hot-pressed specimens. However, the similar phenomenon was observed on the thermal conductivity of the silica-

based ceramic cores. The thermal conductivity of ceramic cores improved up to the SiC content of 10 wt%, in contrast, the thermal conductivity of ceramic core with 20 wt% SiC was reduced due to its microcracks contained air. Consequently, an excessively high content of SiC accelerate crystallization of fused silica, and led to generate microcracks on cristobalite. It is assumed that the microcracks on cristobalite was predominant over prevention of crack propagation on silica-based ceramic cores, and therefore, the mechanical and thermal properties of ceramic core were reduced.

Acknowledgments

This work was supported by the Power Generation & Electricity Delivery Core Technology Program of the Korea Institute of Energy Technology Evaluation and Planning (KETEP), granted financial resource from the Ministry of Trade, Industry and Energy, Republic of Korea (2014101010187B/20141020102460).

References

1. C. Huseby, M.P. Borom, C.D. Greskovich, *Am. Ceram. Soc. Bull.* 58 (1979) 448-452.
2. A.A. Wereszczak, et al., *J. Mater. Sci.* 37[19] (2002) 4235-4245.
3. W.D. Kingery, H.K. Bowen, D.R. Uhlmann, in "Introduction to Ceramics", John Wiley & Sons, U.S.A. (1960) 583.
4. L.C. Carwile, H.J. Hoge, in "Thermal Conductivity Proceedings of Seventh Conference", National Bureau of Standards (NBS) Special Publication 302, U.S.A. (1968) 59-76.
5. A. Kazemi, M.A. Faghihi-Sani, M.J. Nayeri, M. Mohammadi, M. Hajfathalian, *Ceram. Int.* 40[1] (2014) 1093-1098.
6. E.H. Kim, G.H. Cho, Y.S. Yoo, S.M. Seo, Y.G. Jung, *Ceram. Int.* 39[8] (2013) 9041-9045.
7. A.A. Tavassoli, *J. Nucl. Mater.* 302[2] (2002) 73-88.
8. T. Yano, M. Akiyoshi, K. Ichikawa, Y. Tachi, T. Iseki, *J. Nucl. Mater.* 289[1] (2001) 102-109.
9. E.H. Ratcliffe, *Brit. J. Appl. Phys.* 10[1] (1959) 22-25.
10. G.A. Slack, *J. Phys. Chem. Solids.* 34[2] (1973) 321-335.
11. J. Franci, W.D. Kingery, *J. Am. Ceram. Soc.* 37[2] (1954) 99-107.
12. R. Barea, M. Belmonte, M.I. Osendi, P. Miranzo, *J. Eur. Ceram. Soc.* 23[11] (2003) 1773-1778.
13. ASTM C1674-11, ASTM International, West Conshohocken, PA (2011). www.astm.org.
14. ASTM E1461-13, ASTM International, West Conshohocken, PA (2013). www.astm.org.
15. C.J. Bae, "Integrally cored ceramic investment casting mold fabricated by ceramic stereolithography" (Ph.D. Thesis, University of Michigan, Ann Arbor, 2008) 180.
16. M.J. Davis, P.D. Ihinger, *Am. Mineral.* 83[9-10] (1998) 1008-1015.
17. L.Y. Wang, M.H. Hon, *Ceram. Int.* 21[3] (1995) 187-193.
18. A. Kazemi, M.A. Faghihi-Sani, H.R. Alizadeh, *J. Eur. Ceram. Soc.* 33[15] (2013) 3397-3402.
19. R.C. Breneman, J.W. Halloran, *J. Am. Ceram. Soc.* 98[5] (2015) 1611-1617.